



HOCl retrievals from the Atmospheric Chemistry Experiment

P.F. Bernath^{a,b,c,*}, R. Dodandodage^c, C.D. Boone^b, J. Crouse^b

^a Department of Chemistry and Biochemistry, Old Dominion University, Norfolk, VA, 23529, USA

^b Department of Chemistry, University of Waterloo, Waterloo, ON, N2L 3G1, Canada

^c Department of Physics, Old Dominion University, Norfolk, VA, 23529, USA

ARTICLE INFO

Article history:

Received 21 December 2020

Revised 27 January 2021

Accepted 3 February 2021

Available online 7 February 2021

Keywords:

Chlorofluorocarbons

Ozone hole

Satellite remote sensing

Fourier transform spectroscopy

ABSTRACT

HOCl is a chlorine reservoir molecule found in the stratosphere and in the marine boundary layer. In the stratosphere, it originates from anthropogenic emissions of long-lived chlorine-containing molecules as chlorofluorocarbons (CFCs). HOCl is also a key species in polar ozone destruction and the formation of the Antarctic ozone hole. A new HOCl retrieval has been developed using solar occultation spectra recorded by the Atmospheric Chemistry Experiment Fourier Transform Spectrometer (ACE-FTS) from orbit. Altitude-latitude volume mixing ratio (VMR) distributions of HOCl are presented for the entire mission (2004–2020) and for four seasonal quarters. A time series of quarterly averages for the region 60°S–60°N, 35.5–39.5 km altitude shows a marginally significant trend of -0.23 ± 0.11 ppt/year consistent with the success of the Montreal Protocol.

© 2021 Elsevier Ltd. All rights reserved.

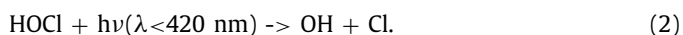
1. Introduction

In 1974, Molina and Rowland [1] found that chlorofluorocarbons (CFCs) are photolyzed in the stratosphere, releasing Cl atoms that destroy O₃ in the ClO_x cycle. Cl reacts with O₃ to make ClO and the Cl atoms are reformed when ClO reacts with O atoms. Ozone in the stratosphere blocks deleterious UV radiation from 200 to 300 nm from reaching the ground. Fortunately, this stratospheric O₃ destruction is mitigated by the formation of Cl-containing “reservoir” compounds such as HCl and ClONO₂ that do not react with O₃ [2].

HOCl (hypochlorous acid) is a relatively minor chlorine-containing reservoir molecule [3] that is formed by the reaction,

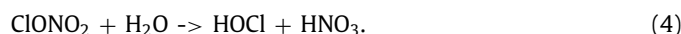
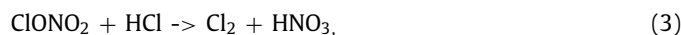


HO₂ originates primarily from the reaction of OH with O₃. Volume mixing ratios (VMRs) of HOCl peak at about 200 ppt in the upper stratosphere just below 40 km for the tropics and mid-latitudes [3]. HOCl shows a substantial diurnal variability [4] from photolysis with wavelengths shorter than 420 nm [5],



Reaction (1) can also form about 100 ppt of HOCl in the marine boundary layer [6], where it is a source of Cl atoms from reaction (2), that destroy O₃ and CH₄.

The most significant atmospheric role for HOCl is during activated chlorine chemistry in the polar stratosphere. In 1985, the discovery of the Antarctic ozone hole [7] spurred the adoption of the Montreal Protocol [8] to control the production of ozone depleting substances such as CFCs. The Antarctic ozone hole forms because the chlorine reservoir molecules ClONO₂ and HCl are converted to molecules such as Cl₂ and HOCl [9] by catalysis on polar stratospheric clouds (PSCs), e.g.,



These heterogeneous reactions start in the cold polar night and when sunlight returns in the spring, photolysis converts Cl₂ and HOCl to Cl atoms, which then form ClO by reaction with O₃. Catalytic O₃ destruction, however, does not proceed by the ClO_x cycle because the O atom abundance is too low, but through the formation of the ClO dimer, ClOCl [2]. Nakajima et al. [10] calculate that the HOCl abundance peaks at about 500 ppt in the Antarctic lower stratosphere.

Recently Müller et al. [11] demonstrated the importance of “HCl null cycles” that involve HOCl in maintaining rapid ozone destruction in the Antarctic spring. In the spring, HCl is rapidly reformed by the reaction of Cl with CH₄, which if not counteracted would end O₃ destruction in a few days. These null cycles involve the for-

* Corresponding author.

E-mail address: pbernath@odu.edu (P.F. Bernath).

mation of HOCl by reaction (1), followed by the heterogeneous reaction catalyzed by PSCs,



Reaction (5) converts the HCl reservoir molecule back into the active Cl_2 molecule, which maintains the destruction of O_3 for several months in the Antarctic spring.

Atmospheric HOCl has been measured by infrared spectroscopy with instruments on aircraft, balloons and satellites. Toon and Farmer [12] determined the total column above an aircraft in September 1987 in the Antarctic ozone hole. Altitude profiles of HOCl near Palestine, Texas were determined by Chance et al. [13] using far-infrared rotational emission spectroscopy. Kovalenko et al. [14] observed HOCl profiles in the mid-latitude stratosphere with two balloon-borne instruments: a far-infrared emission spectrometer (FIRS-2), and a mid-infrared solar occultation spectrometer (MkIV). Based on a comparison between model predictions and observations, they were able to validate the rate constant for reaction (1).

The most comprehensive HOCl measurements were made by the MIPAS (Michelson Interferometer for Passive Atmospheric Sounding) limb emission Fourier transform spectrometer on ENVISAT [3,15,16]. The vibration-rotation lines of the ν_2 bending mode near 1238 cm^{-1} [17] were used by von Clarmann et al. [15] to retrieve HOCl VMRs between about 20 and 50 km. MIPAS made HOCl measurements in the Antarctic polar vortex of 2002 [16] and von Clarmann et al. [3] published a climatology for 2002–2004. The Microwave Limb Sounder (MLS) on Aura and the Superconducting Submillimeter-wave Limb-Emission Sounder (SMILES) on the International Space Station have an HOCl data product based on rotational transitions near 630 GHz. The MLS product requires considerable averaging before it can be used [18]; the SMILES measurements had a higher signal-to-noise ratio than MLS because it used a more sensitive detector [19]. HOCl observations from SMILES were also used to evaluate the rate constant for reaction (1) [20], to measure the diurnal variation [4] and for an equatorial climatology [21].

We report on a new HOCl data product retrieved from solar occultation spectra recorded with the ACE-FTS from orbit [22]. These altitude VMR profiles cover the period from 2004 to 2020. As part of monitoring the Montreal Protocol, it is important to measure the long-term abundance trends of chlorine-containing molecules such as HOCl. Currently ACE-FTS and MLS are the only instruments capable of providing these data.

2. Observations and data retrievals

The Atmospheric Chemistry Experiment (ACE), also known as SCISAT, is a satellite mission launched by NASA on 12 August 2003 [22]. The original goal of ACE was to study the atmospheric chemistry and dynamics associated with stratospheric ozone depletion; now with more than 17 years on orbit, ACE data are also being used to measure changes in atmospheric composition [23]. The satellite orbit is a near-circular orbit at an altitude of 650 km with an inclination of 73.9° to the equator. It is a limb sounder with an orbital period of 97.6 min capable of recording up to 30 occultations per day, measuring atmospheric absorption spectra during sunset and sunrise.

The primary instrument is the high-resolution Fourier Transform Spectrometer (ACE-FTS) operating in the $750 - 4400 \text{ cm}^{-1}$ region with a spectral resolution of 0.02 cm^{-1} . The most recent ACE-FTS processing version (4.1) provides VMR altitude profiles for 44 molecules and 24 subsidiary isotopologues [24].

HOCl retrievals involve the analysis of microwindows: selected spectral regions containing the strongest HOCl absorption with

Table 1
Microwindow set for HOCl retrieval.

Microwindow center (cm^{-1})	Microwindow width (cm^{-1})	Lower altitude limit (km)	Upper altitude limit (km)
1228.2	7.5	$17 - 4\sin^2(\text{latitude})$	40
1246.79	4.5	$17 - 4\sin^2(\text{latitude})$	40
1251.75	5.5	$17 - 4\sin^2(\text{latitude})$	40
1257.25	5.5	$17 - 4\sin^2(\text{latitude})$	40
1483.19 ^a	0.3	$17 - 4\sin^2(\text{latitude})$	25

^a Microwindow to improve results for interferer H_2^{18}O

minimal systematic residuals from interferers (i.e., absorption features from species other than the target molecule), an important consideration for a weak absorber like HOCl. The set of microwindows employed in HOCl retrievals is presented in Table 1. A lower limit that varies with latitude is used to avoid large systematic residuals from interfering H_2O lines that would occur in the tropical troposphere [25], yielding an altitude range of 17 to 40 km at the equator and ~ 14 to 40 km near the poles. An additional microwindow is employed to stabilize the retrieval for one of the interferers (H_2^{18}O), which has weak absorption in the main microwindow set.

Altitude profiles for HOCl VMR are generated through a non-linear least-squares global fitting of the microwindow regions in Table 1 for all measurements having tangent heights falling in the given altitude range. VMR profiles are simultaneously determined for the target molecule (HOCl) and all interfering species contributing to the spectrum in the microwindow regions, in order to minimize systematic errors from the interferers. Independent VMR profiles are used for different isotopologues of a particular molecule to account for isotopic fractionation. The interferers in the HOCl retrieval are H_2O , H_2^{18}O , HDO, ^{18}OCO , ^{17}OCO , O_3 , N_2O , N^{15}NO , ^{15}NNO , N_2^{18}O , N_2^{17}O , CH_4 , $^{13}\text{CH}_4$, CH_3D , H_2O_2 , COF_2 , and N_2O_5 .

The retrievals used temperature, pressure, and tangent height information from ACE-FTS version 4.1 retrievals [24]. Spectroscopic data comes primarily from HITRAN 2016 [26], where the source of HOCl information in this line list is Vander Auwera et al. [17]. CH_4 and N_2O lines in the microwindow regions suffer significant systematic residuals when using the standard Voigt line shape. Therefore, to minimize residuals from these interferers, speed-dependent Voigt parameters were derived for N_2O in this spectral region, along with a combination of speed-dependent Voigt and line mixing parameters for CH_4 [24].

Fig. 1a shows the calculated and observed spectra obtained for the first microwindow from Table 1 in the HOCl retrieval for occultation sr86147 (where sr stands for sunrise and 86147 is the number of orbits since launch, the combination of which is a unique identifier for the occultation). Fig. 1b shows the residuals (in orange). This occultation, which occurred within the Antarctic polar vortex (latitude 67.5°S) on August 9th, 2019, exhibits a strong enhancement in HOCl, a common occurrence for winter/spring in the Antarctic, as a consequence of chlorine processing [16]. For the measurement in Fig. 1, HOCl has a peak absorption of approximately 5%, as indicated by the difference between the curves with and without HOCl included in the calculation shown in Fig. 1b. This is a best-case example that has the one of the largest HOCl VMRs measured by ACE.

Note that the residuals with HOCl included in Fig. 1b are not completely flat because of a polar stratospheric cloud (PSC) in the field-of-view. The PSC contributing to the spectrum is missing from the calculation. However, there is little structure in the PSC spectrum in this region, and the bulk of its spectral contribution is captured by the simple baseline parameters (baseline scaling and baseline slope) always used in the least-squares fitting. The small

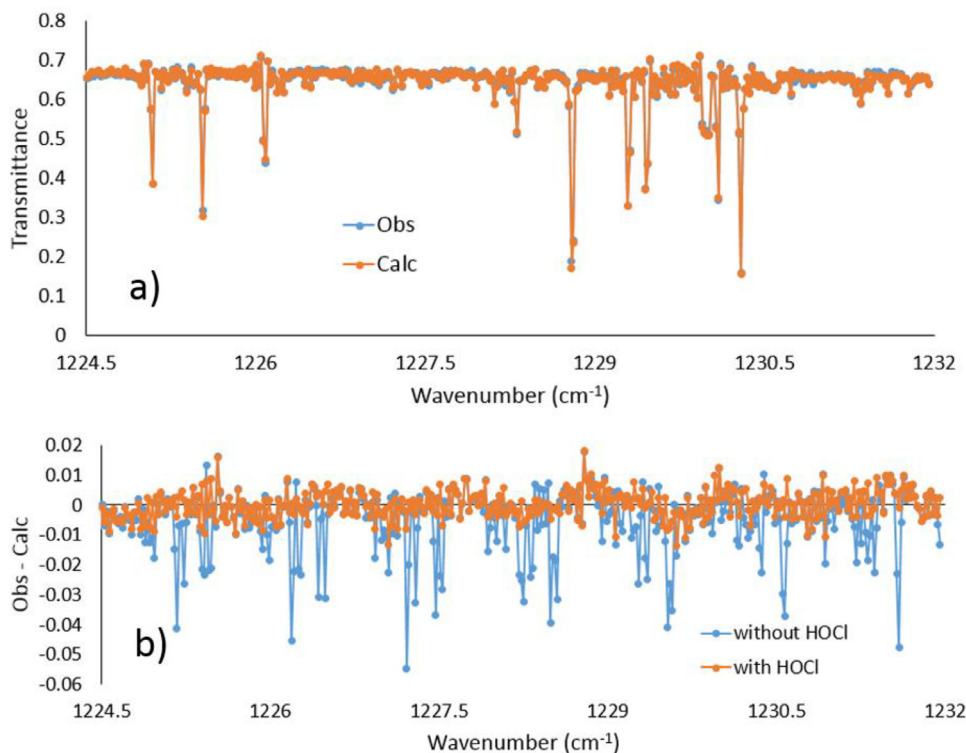


Fig. 1. a) Observed (in blue) and calculated (in orange) spectra from a measurement at tangent height 22.3 km from occultation sr86147. The strong lines are due to CH₄ and H₂O. b) Fitting residuals (observed – calculated) without HOCl included in the calculated spectrum shown in blue and with HOCl included shown in orange.

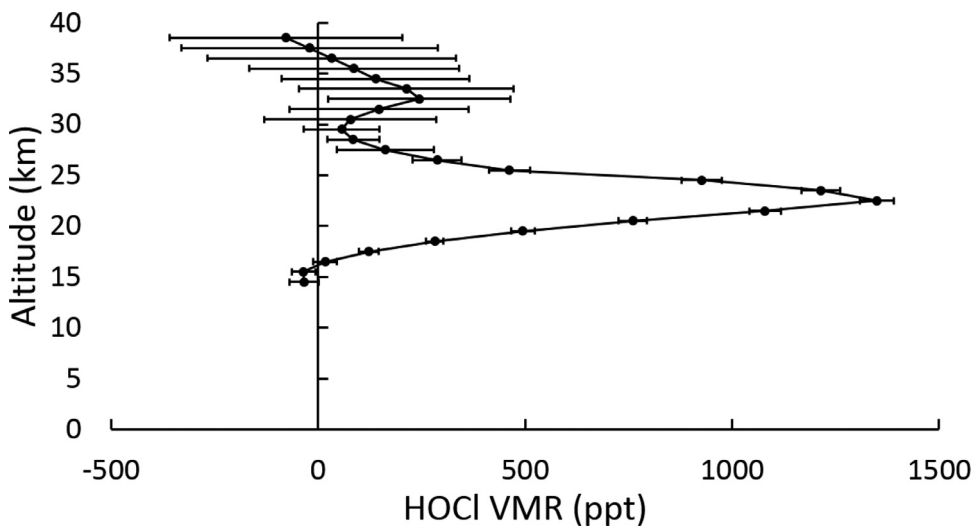


Fig. 2. HOCl VMR profile for sr86147 (9 August 2019, 67.5°S, 99.5°W).

broad features in the baseline do not affect the HOCl retrieval that is based on sharp vibration-rotation lines.

The HOCl altitude profile for sr86147 (9 August 2019, 67.5°S, 99.5°W), associated with Fig. 1 is displayed in Fig. 2. The peak VMR is a remarkable 1.34 ± 0.06 ppb at an altitude of 22.5 km. Typically in August, HOCl has values around 400 ppt with occasional enhancements to 600 or 800 ppt in the Antarctic polar vortex. The degree of HOCl enhancement in August varies from year to year with 2019 being particularly large. In Fig. 2, the usual stratospheric HOCl peak near about 40 km (see discussion below) has descended to 32.5 km and has a value of 255 ± 231 ppt. The vertical resolution of the HOCl profile in Fig. 2 is about 3 km, limited by the vertical sampling.

Outside of Antarctic winter/spring, the HOCl signal is typically fairly weak, but the retrieval is helped by the relatively high density of HOCl lines in the microwindows and the high signal-to-noise ratio for the ACE-FTS instrument for all of the wavenumber regions used for the retrieval (> 300:1). The retrieval approach does not use optimal estimation or explicit smoothing, and so the upper altitude limit in the retrieval was set to 40 km to avoid excessive variability encountered above that altitude in preliminary studies. The HOCl retrieval provides a statistical error for each VMR value. Typical errors for a single occultation start at about 30 ppt at 15 km and increase steadily with altitude up to about 150–200 ppt at 40 km; for mid-latitudes the fractional errors are therefore greater than 100% below about 30 km and just under 100% from 30

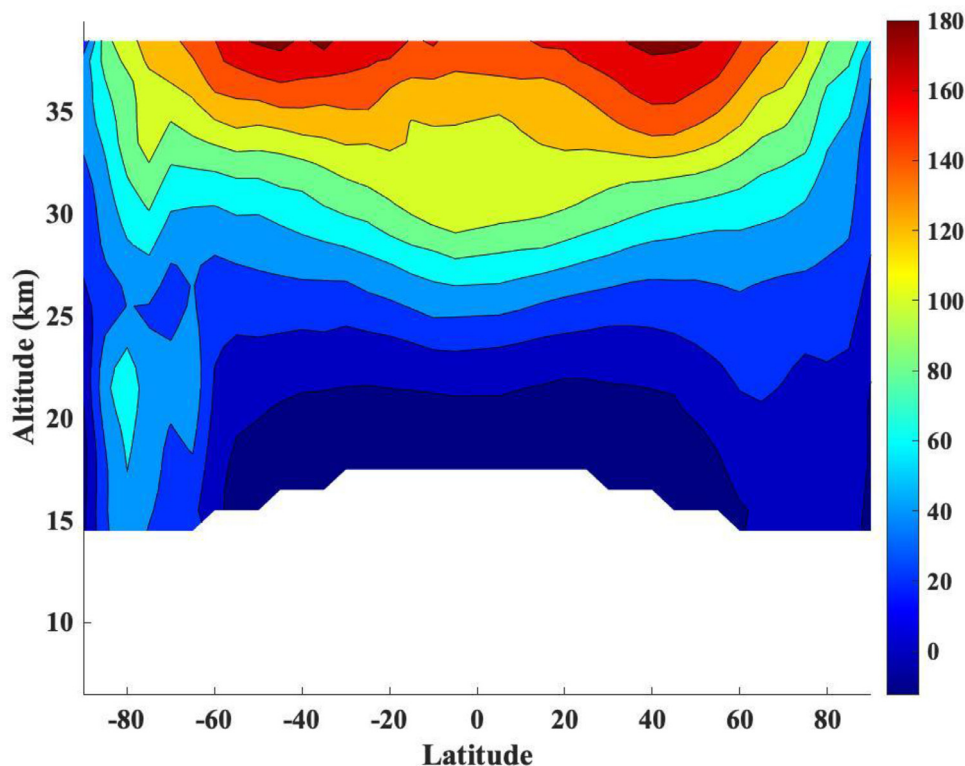


Fig. 3. HOCl altitude-latitude VMR plot for the 2004-2020 mission average. The x-axis is in degrees and the color scale is HOCl VMR (ppt).

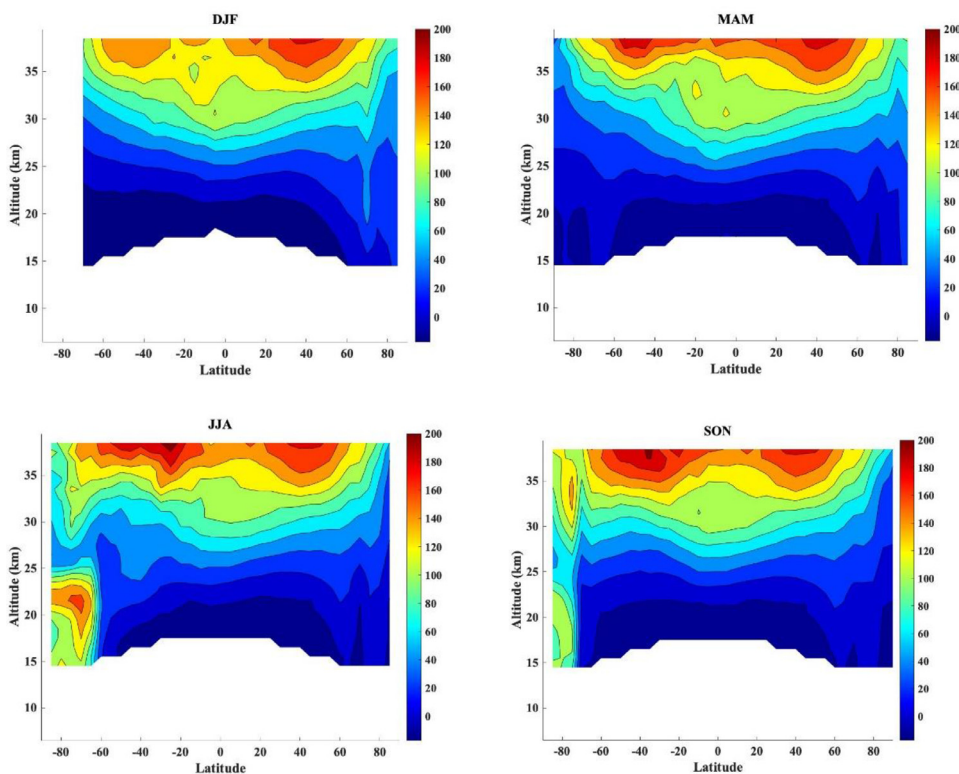


Fig. 4. Quarterly average VMR altitude-latitude distributions. The x-axis is in degrees and the color scale is in ppt.

to 40 km. Systematic errors are difficult to estimate but the error code in HITRAN for the HOCl line strengths corresponds to 5-10% error.

The data reported here represent a ‘research product’, but HOCl will become a routine data product in the upcoming ACE-FTS processing version 5.0.

3. Results and discussion

The retrieved HOCl VMR values from Feb. 2004 to Aug. 2020 were separated into 5° latitude bins at each altitude from 14.5 km to 39.5 km. VMR values less than -300 ppt and greater than 1500 ppt were filtered out to remove unphysical values. The mission av-

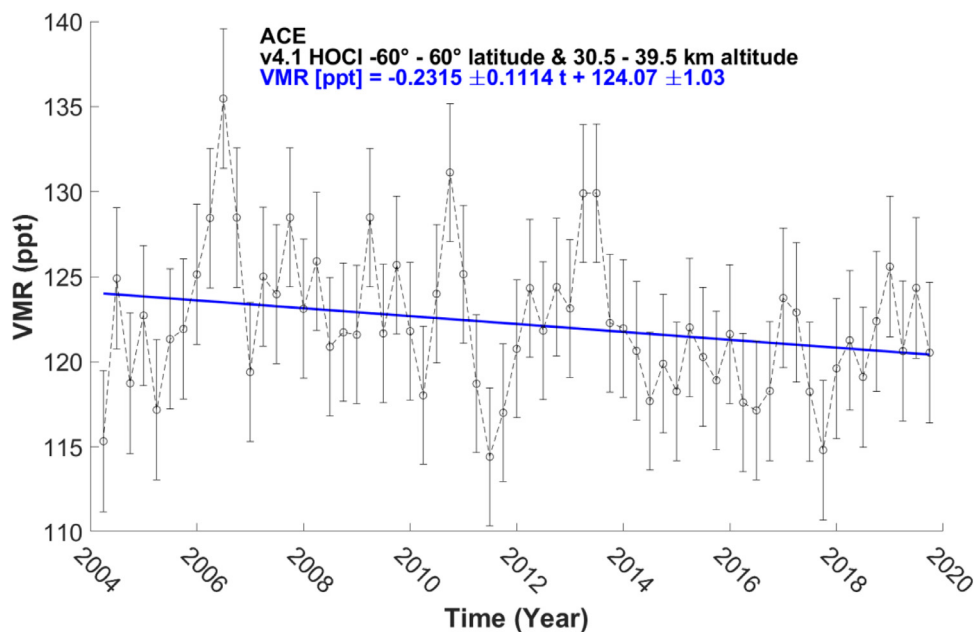


Fig. 5. Quarterly HOCl time series for 60°S-60°N from 30.5-39.5 km in altitude.

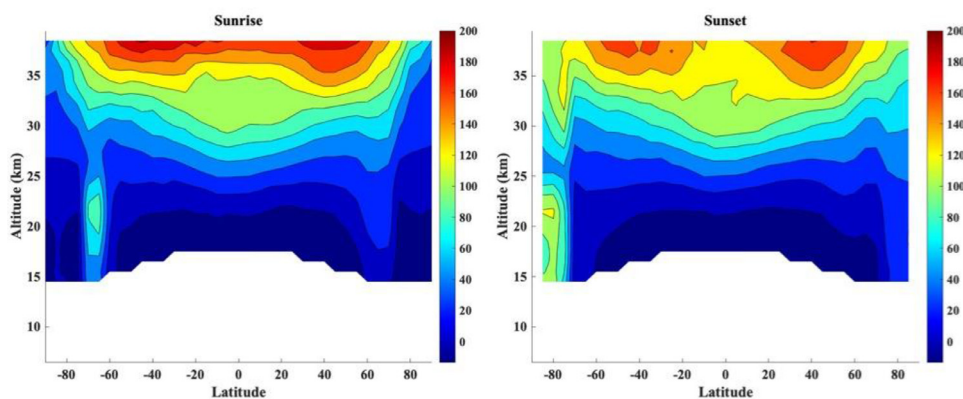


Fig. 6. Mission average altitude-latitude HOCl VMR distributions for sunrise (left) and sunset (right) occultations. The x-axis is in degrees and the color scale is in ppt.

erage values are illustrated in the altitude-latitude plot in Fig. 3. Data from 97120 occultation profiles corresponding to more than 2 million points were used to generate Fig. 3.

In Fig. 3, the mid-latitude peaks are about 160 ppt near 40 km in altitude around 40°S and 40°N latitude. These peak values are less than the 200 ppt peaks seen by MIPAS near 30°N and 35°N during the day and the night [15]. SMILES also finds HOCl peaks of 150-180 ppt just above 40 km at night and just below 40 km during the day [21]. ACE-FTS measurements are at twilight and have solar zenith angles near 90°. In addition, there are HOCl features near 80°S and 30-35 km associated with descent in the Antarctic polar vortex, seen more clearly in the quarterly plots below. A feature at near 80°S and 18-23 km that is caused by HOCl production on PSCs is present.

The HOCl VMR values were separated into four different quarters: DJF (December, January, February), MAM (March, April, May), JJA (June, July, August), and SON (September, October, November). The global sampling by ACE [22] biases the results and the quarterly distributions are only approximately seasonal distributions. ACE measurements are mainly at high latitudes (see Fig. 6 in ref. [22] for details) with some relatively brief mid-latitude and tropical measurements about every 2 months. Therefore, each quarterly distribution is based mainly on polar data with a small con-

tribution from mid-latitude and tropical measurements. The average VMR value in each altitude-latitude bin for each quarter is illustrated in Fig. 4. HOCl descent in the Arctic vortex and Arctic polar chemistry is now visible near 70°N in DJF; the corresponding Antarctic features are visible for both JJA and SON quarters. As expected, chlorine activation is much less in the Arctic than in the Antarctic, and this is reflected in the strongly enhanced HOCl in the Antarctic ozone hole compared to the very small enhancements in the Arctic. The occasional strongly enhanced HOCl VMR (Fig. 2) is confined mainly to the Antarctic polar vortex. However, ozone depletion was particularly strong in spring 2020 in the Arctic [27] and a strongly enhanced HOCl VMR profile was observed 11 Feb. 2020 at 68.0°N, 70.6°E with a peak VMR of 1.25 ± 0.06 ppb at 20.5 km in altitude.

ACE has data from Feb. 2004, so it may be possible to determine a VMR trend. Since HOCl VMRs peak in the upper stratosphere, a quarterly time series was created using all values 60°S to 60°N from 30.5 km to 39.5 km in altitude. These values were averaged for each quarter starting from MAM 2004 to JJA 2020. The HOCl time series is depicted in Fig. 5 and a linear trend was fitted using the same methodology as in the v4.0 [23] and v4.1 [28] trend analysis. HOCl shows a decreasing trend of -0.23 ± 0.11 ppt/year, which is marginally significant. HOCl is expected to de-

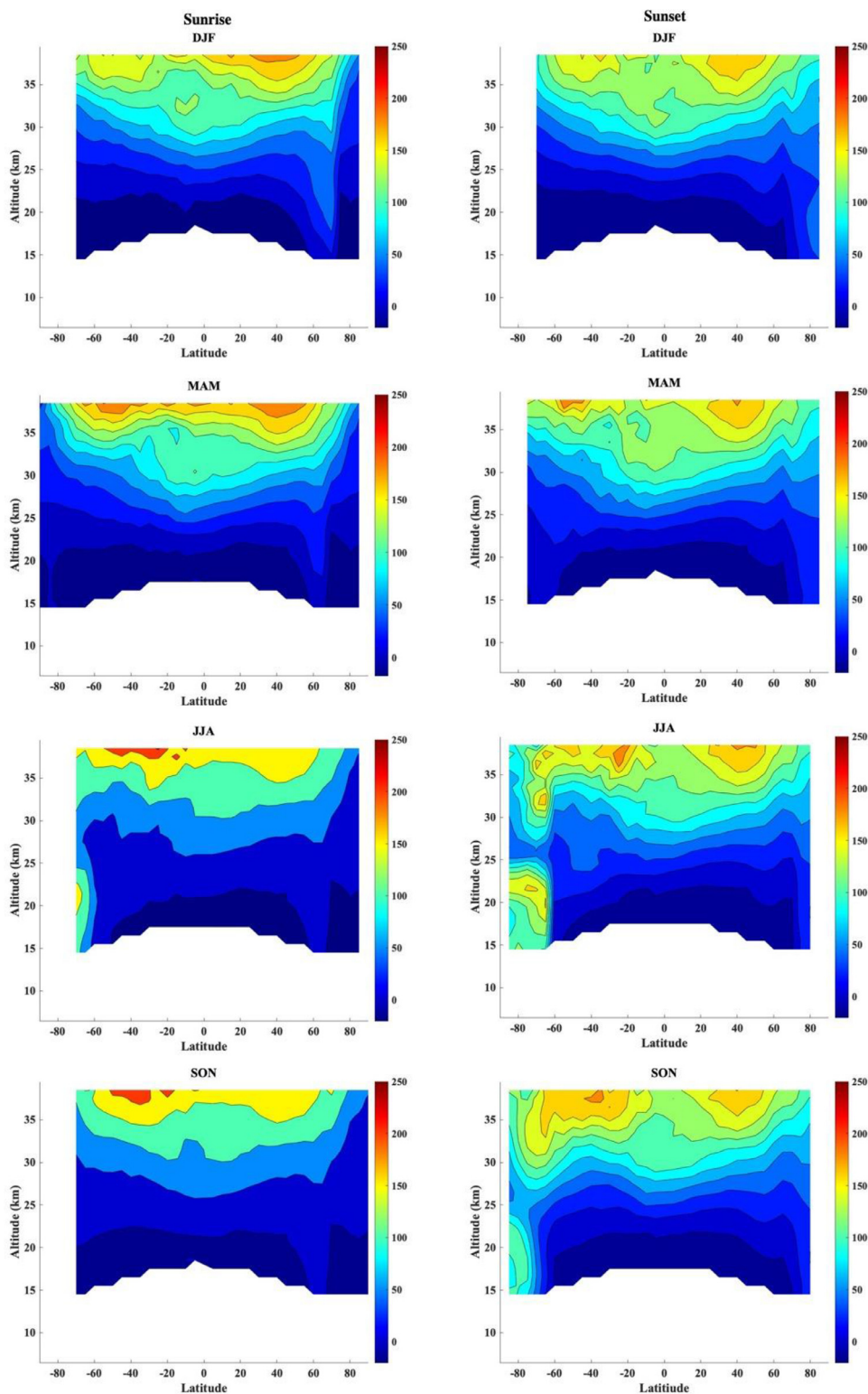


Fig. 7. Mission average quarterly altitude-latitude HOCl VMR distributions for sunrise (left) and sunset (right) occultations. The x-axis is in degrees and the color scale is in ppt.

crease because of the success of the Montreal Protocol in reducing the chlorine burden in the stratosphere [29]. The change in HOCl VMR is about -0.2%/year compared to the change in stratospheric HCl of about -0.5%/year [29].

The rapid photolysis of HOCl, reaction (2), causes a substantial diurnal (more correctly, diel) VMR variation [4] suggesting that

sunrise and sunset occultations may give different altitude-latitude distributions. Fig. 6 shows the mission average sunrise and sunset distributions. The quarterly altitude-latitude distributions show similar differences in Fig. 7. In Figs. 6 and 7, many of the differences are from the different spatial sampling distributions for sunrises and sunsets in the quarter. Sunrise occultations and sun-

set occultations are almost always sampling different hemispheres [22]. For example, as illustrated by Fig. 6 in ref. [22], in SON the sunrises sample the Northern Hemisphere in September and October, switching to the Southern Hemisphere in November; sunsets sample the Southern Hemisphere for September and half of October, then switch to the Northern Hemisphere for the second half of October and November.

ACE HOCl retrievals have been compared with other measurements. For example, the value observed by MkIV at 37 km is about 170 ppt [14] compared to the ACE VMR of 169 ppt at 37.5 km in the SON quarter for the 35°–40°N latitude bin. Note, however, both values have large statistical errors. MIPAS measurements of HOCl averaged over 18 – 27 Sept. and 11 – 13 Oct. 2002 at 35°N peak at 180 ppt during the night at 37 km and at 200 ppt during day at 35 km [15]. MLS VMR measurements of HOCl averaged over Nov. 2009 to Apr. 2010 in the latitude range 20°S to 20°N at 35 km are around 153 ppt [4]. For SMILES during March–April 2010, for the zonal range of 20°S–20°N, the nighttime VMRs peak at about 150 ppt at 42 km and the daytime VMRs peak at about 160 ppt at 38 km [21]. ACE-FTS measurements averaged from Sept.–Nov. 2004–2020, range from 158 ppt to 186 ppt from 35.5 km to 37.5 km in altitude.

4. Conclusion

A new HOCl data product has been determined from solar occultation spectra recorded by the ACE-FTS from 2004–2020. Global altitude–latitude distributions show VMR peaks in the upper stratosphere and enhanced HOCl abundances during Antarctic ozone depletion. A time series of quarterly averages for the region 60°S–60°N, 30.5–39.5 km altitude shows a marginally significant trend of -0.23 ± 0.11 ppt/year consistent with the success of the Montreal Protocol. With the addition of HOCl, the ACE mission provides a very comprehensive set of observations of nearly all of the major species involved in polar ozone chemistry: O₃, HCl, ClONO₂, HOCl, NO₂, ClO, CH₄, HNO₃, H₂O and even H₂CO, which is important in HCl null cycles [11] that maintain the concentration of active chlorine species. In particular, ACE data allow detailed evaluation of polar ozone chemistry modeling as presented for example by Müller et al. [11]. The ACE-FTS HOCl research product is available from the authors upon request.

Declaration of Competing Interest

The authors declare that they have no known competing financial interests or personal relationships that could have appeared to influence the work reported in this paper.

CRedit authorship contribution statement

P.F. Bernath: Writing – original draft, Supervision. **R. Dodandodage:** Writing – review & editing, Formal analysis, Visualization. **C.D. Boone:** Data curation, Writing – review & editing, Software. **J. Crouse:** Data curation, Writing – review & editing.

Acknowledgments

The ACE satellite mission is funded by the [Canadian Space Agency \(9F045-180032/001/MTB\)](https://www.space.gc.ca/9F045-180032/001/MTB).

References

- [1] Molina MJ, Rowland FS. Stratospheric sink for chlorofluoromethanes chlorine atomic-catalysed destruction of ozone. *Nature* 1974;249:810–12.
- [2] Solomon S. Stratospheric ozone depletion: a review of concepts and history. *Rev Geophys* 1999;37:275–316.
- [3] von Clarmann T, Funke B, Glatthor N, Kellmann S, Kiefer M, Kirner O, et al. The MIPAS HOCl climatology. *Atmos Chem Phys* 2012;12:1965–77.

- [4] Khosravi M, Baron P, Urban J, Froidevaux L, Jonsson A, Kasai Y, et al. Diurnal variation of stratospheric and lower mesospheric HOCl, ClO and HO₂ at the equator: comparison of 1-D model calculations with measurements of satellite instruments. *Atmos Chem Phys* 2013;13:7587–606.
- [5] Hickson KM, Keyser LF, Sander SP. Temperature dependence of the HO₂+ClO reaction. 2. Reaction kinetics using the discharge–flow resonance–fluorescence technique. *J Phys Chem A* 2007;111:8126–38.
- [6] Lawler M, Sander R, Carpenter L, Lee J, Von Glasow R, Sommariva R, Saltzman E. HOCl and Cl₂ observations in marine air. *Atmos Chem Phys* 2011;11:7617–28.
- [7] Farman J, Gardiner B, Shanklin J. Large losses of total ozone in Antarctica reveal seasonal ClO_x/NO_x interaction. *Nature* 1985;315:207–10.
- [8] Montreal Protocol on Substances that Deplete the Ozone Layer, 1987; <http://ozone.unep.org/en/treaties-and-decisions/montreal-protocol-substances-deplete-ozone-layer>.
- [9] Solomon S, Garcia RR, Rowland FS, Wuebbles DJ. On the depletion of Antarctic ozone. *Nature* 1986;321:755–8.
- [10] Nakajima H, Murata I, Nagahama Y, Akiyoshi H, Saeki K, Kinase T, et al. Chlorine partitioning near the polar vortex edge observed with ground-based FTIR and satellites at Syowa Station, Antarctica, in 2007 and 2011. *Atmos Chem Phys* 2020;20:1043–74.
- [11] Müller R, Grooss J-U, Zafar AM, Robrecht S, Lehmann R. The maintenance of elevated active chlorine levels in the Antarctic lower stratosphere through HCl null cycles. *Atmos Chem Phys* 2018;18:2985–97.
- [12] Toon G, Farmer C. Detection of HOCl in the Antarctic stratosphere. *Geophys Res Lett* 1989;16:1375–7.
- [13] Chance K, Johnson D, Traub W. Measurement of stratospheric HOCl: Concentration profiles, including diurnal variation. *J Geophys Res* 1989;94:11059–69.
- [14] Kovalenko L, Jucks K, Salawitch R, Toon G, Blavier J-F, Johnson D, et al. Observed and modeled HOCl profiles in the midlatitude stratosphere: implication for ozone loss. *Geophys Res Lett* 2007;34:L19801.
- [15] von Clarmann T, Glatthor N, Grabowski U, Höpfner M, Kellmann S, Linden A, et al. Global stratospheric HOCl distributions retrieved from infrared limb emission spectra recorded by the Michelson Interferometer for Passive Atmospheric Sounding (MIPAS). *J Geophys Res* 2006;111:D05311.
- [16] von Clarmann T, Glatthor N, Ruhnke R, Stiller G, Kirner O, Reddmann T, et al. HOCl chemistry in the Antarctic Stratospheric Vortex 2002, as observed with the Michelson Interferometer for Passive Atmospheric Sounding (MIPAS). *Atmos Chem Phys* 2009;9:1817–29.
- [17] Vander Auwera J, Kleffmann J, Flaud J-M, Pawelke G, Bürger H, Hurtmans D, Petrisse R. Absolute ν_2 line intensities of HOCl by simultaneous measurements in the infrared and far infrared spectral regions. *J Mol Spectrosc* 2000;204:36–47.
- [18] Livesey NJ, Read W.G., Wagner P.A., Froidevaux L., Santee M.L., Schwartz M.J., et al. EOS Aura MLS, Version 5.0x Level 2 and 3 data quality and description document. JPL D-105336, Version 5.0-1.0a, June 1, 2020.
- [19] Baron P, Urban J, Sagawa H, Möller J, Murtagh DP, Mendrok J, et al. The level 2 research product algorithms for the Superconducting Submillimeter-Wave Limb-Emission Sounder (SMILES). *Atmos Meas Tech* 2011;4:2105–24.
- [20] Kuribayashi K, Sagawa H, Lehmann R, Sato T, Kasai Y. Direct estimation of the rate constant of the reaction ClO + HO₂ → HOCl + O₂ from SMILES atmospheric observations. *Atmos Chem Phys* 2014;14:255–66.
- [21] Kreyling D, Sagawa H, Wohltmann I, Lehmann R, Kasai Y. SMILES zonal and diurnal variation climatology of stratospheric and mesospheric trace gases: O₃, HCl, HNO₃, ClO, BrO, HOCl, HO₂, and temperature. *J Geophys Res* 2013;118:11888–903.
- [22] Bernath P. The Atmospheric Chemistry Experiment (ACE). *J Quant Spectrosc Rad Transf* 2017;186:3–16.
- [23] Bernath PF, Steffen J, Crouse J, Boone CD. Sixteen-year trends in atmospheric trace gases from orbit. *J Quant Spectrosc Rad Transf* 2020;253:107178.
- [24] Boone CD, Bernath PF, Cok D, Steffen J, Jones SC. Version 4 retrievals for the Atmospheric Chemistry Experiment Fourier Transform Spectrometer (ACE-FTS) and Imagers. *J Quant Spectrosc Rad Transf* 2020;247:106939.
- [25] Boone CD, Walker KA, Bernath PF. Speed-dependent Voigt profile for water vapor in infrared remote sensing applications. *J Quant Spectrosc Radiat Transf* 2007;105:525–32.
- [26] Gordon IE, Rothman LS, Hill C, Kochanov RV, Tan Y, Bernath PF, et al. The HITRAN 2016 molecular spectroscopic database. *J Quant Spectrosc Radiat Transf* 2017;203:3–69.
- [27] Manney GL, Livesey NJ, Santee ML, Froidevaux L, Lambert A, Lawrence ZD, et al. Record low Arctic stratospheric ozone in 2020: MLS observations of chemical processes and comparisons with previous extreme winters. *Geophys Res Lett* 2020;47 e2020GL089063.
- [28] Bernath PF, Crouse J, Hughes RC, Boone CD. The Atmospheric Chemistry Experiment Fourier Transform Spectrometer (ACE-FTS) version 4.1 retrievals: trends and seasonal distributions. *J Quant Spectrosc Rad Transf* 2021;259:107409.
- [29] Bernath P, Fernando AM. Trends in stratospheric HCl from the ACE satellite mission. *J Quant Spectrosc Rad Transf* 2018;217:126–9.